Desalination and Water Treatment
www.deswater.com

doi:10.5004/dwt.2018.23145

135 (2018) 279–289
December

Development of a high efficiency rice husk based adsorbent for removal of dyes from wastewater: application to Everzol Black GR and Reactive Orange 113

Yumna Sadef[a,*], Tjalfe G. Poulsen[b], Javed Iqbal[c], Misbah Noureen[a,*], Nusrat Afzal[f], Irfan Ahmed Shaikh[a]

[a]*College of Earth and Environmental Sciences, University of the Punjab, 54000 Lahore, Pakistan, email: yumna.sadef@gmail.com. (Y. Sadef), anzalnahh@gmail.com (M. Noureen), textilemaster@gmail.com (I.A. Shaikh)*
[b]*Department of Chemical Engineering, Guangdong Technion Israel Institute of Technology, 15000 Shantou, China, email: tjalfe.poulsen@gtiit.edu.cn, ragnerlodbrog@hotmail.com (T.G. Poulsen)*
[c]*Center for Environmental Protection Studies, Pakistan Council of Scientific and Industrial Research Laboratories Complex, 54000 Lahore, Pakistan, email: javedchemist13@gmail.com (J. Iqbal), hanyia.afzal@yahoo.com (N. Afzal)*

Received 9 October 2017; Accepted 17 September 2018

ABSTRACT

Rice husk is a type of bio-waste that is easily available and provides a base for formation of an effective adsorbent along with chitosan. ZnO-coated chitosan carbonized rice husk (ZnO-CCRH) was prepared by blending Zn-loaded chitosan with rice husk. The adsorbent was then applied to remove color from wastewater. Different isothermal, kinetic and thermodynamic models were applied to evaluate adsorbent efficiency. Results showed that adsorption capacity for two dyes Everzol Black Gr (EBG) and Reactive Orange 113 (RO113) onto ZnO-CCRH was best described by the Langmuir model. Adsorption appeared to follow the mono layer adsorption mechanism, likely because the adsorbent (ZnO-CCRH) has heterogeneous surfaces. In case of adsorption kinetics,results indicated that the pseudo-second-order kinetic model best described the adsorption of EBG and RO 113 onto ZnO coated chitosan carbonize rice husk. Furthermore, thermodynamic studies also revealed exothermic adsorption process for the said dyes. The adsorbent was further characterized by FTIR, SEM and X-Ray diffraction. Results of the characterization indicated that the ZnO-CCRH adsorbent has a strong potential for color removal.

Keywords: Carbonized rice husk; Adsorption modeling; Chitosan; Reactive dyes; Wastewater

1. Introduction

Textile industry consumes relatively large quantities of water for the dyeing process, which subsequently results in production of substantial quantities of wastewater containing surplus dye and other processing chemicals. These contaminants potentially cause carcinogenicity and mutagenicity in aquatic organisms as well as in humans if the wastewater contaminates drinking water sources [1,2]. Microbial degradation of the contaminants may further cause oxygen depletion and the contaminants may reduce light penetration into the water affecting both plant and animal life. Certain types of dyes (e.g. azo dyes) can persist for long periods of time after discharge into the environment due to the presence of aromatic ring structures in their molecules,which makes them resistant to degradation. In addition both the dyes themselves, and many of their degradation products are toxic to many aquatic organisms. These compounds may also cause allergic reactions and skin cancer in humans [3,4]. Global dye chemical consumption is approximately 700.000 ton/y of which azo dyes account for about 50% [5]. The wastewater produced by the textile industry is usually rich in color along with high values of chemical oxygen demand (COD), complex chemicals, inorganic salts and total dissolved solids (TDS), pH, temperature, turbidity and salinity [6].

*Corresponding author.

The most problematic class of dyes found in textile effluents is called reactive dyes. Reactive dyes are molecules containing specific functional groups, which react with other functional groups present on the fibers to be dyed, forming covalent dye-fiber bonds. They are available in a wide range of bright shades, have excellent water resistance with minimum color loss during washing and excellent grades for the staining of white goods. Significant quantities of dye are normally lost with wastewater during the process. For instance almost 50% of reactive dyes may be lost with the effluents during dyeing of cellulose fibers [7]. An additional 10–20% of reactive dyes are lost with the wastewater during dye production due to the very high water solubility of reactive dyes [8]. In an aerobic environment as found in traditional wastewater treatment plants, these dyes have very low biodegradability. Under anaerobic conditions, however, many azo dyes decompose readily into aromatic amines, which are potential carcinogens. Thus, traditional aerobic or anaerobic biological treatment methods are inadequate for removing these types of contaminants from wastewater.

A well-known, efficient and commercially available alternative method for dye removal is adsorption. This process has become widely used due to its simplicity, sludge free operation and easy handling [9]. Various conventional and non-conventional adsorbent materials have been studied for their application in dye removal [10–12]. Bio-sorbent materials, such as fungal or bacterial biomass and biopolymers have gained significant attention [13,14]. Bamboo-based activated carbon have been used successfully for the removal of azo dyes [15,16] Bone char produced by the calcination of cattle bones at 1000°C in the absence of oxygen has also shown a good adsorption capacity for metal ions such as cadmium, copper and zinc [17].

Chitosan, a biopolymer of glucosamine has received increased interest for removal of transition metal ions and organic compounds due to its excellent metal chelating properties [18], absence of toxicity and biodegradability [19]. In acidic media, chitosan has a high capacity for adsorption of anionic dyes [18,20]. It contains hydroxyl and amino groups that chelate with heavy metals, recovering them from aqueous solution [21,22]. For an efficient adsorption process and easy handling of sorbed contaminants, chitosan, however, needs to be attached to a carrier material such as carbonized biomass. Rice husk is an inexpensive and readily available biomass material containing silica (20%), cellulose (40%), hemicellulose (20%) and lignin content (20%) [23]. Rice husk may therefore, potentially serve as a carrier material for chitosan during dye adsorption.

In a previous study [24] carbonized rice husk was used as carrier material to produce an adsorbent based on Fe-loaded chitosan (Fe-loaded chitosan carbonized rice husk, Fe-CCRH). This adsorbent was further studied with respect to its adsorption characteristics with respect to the removal of metal ions. Rice husk has also been used for organic pollutant removal [25]. Rice husk, which is a relatively abundant and inexpensive material, is currently being investigated as an adsorbent for the removal of various pollutants from water and waste waters. Various pollutants, such as dyes, phenols, organic compounds, pesticides, inorganic anions, and heavy metals can be removed very effectively with rice husk as an adsorbent. [26]. Removal of methylene blue from wastewater was investigated by using rice husk activated carbon and found 97% removal of dye [27]. Direct Red dye was also removed effectively using rice husk adsorption [28].

Zn has many of the same chemical characteristics as Fe, however, at present the efficiency of chitosan in combination with Zn as an adsorbent has not been investigated. Consequently, very little is known about the efficiency of this type of adsorbent.

The objectives of the present study are therefore: 1) to prepare a cost effective and environmentally friendly bio sorbent *i.e.*, ZnO coated chitosan carbonized rice husk, for removal of Reactive orange 113 (RO113) and Everzol Black Gr (EBG) dyes present in wastewater. 2). To investigate the influence of experimental conditions such as initial dye concentration, solution pH, temperature, contact time and shaking speed on process efficiency. Experimental measurements of sorption capacity are compared to the Langmuir, Freundlich and Temkin adsorption isotherm models. The kinetics of the adsorption process is further investigated using first and second order kinetic models.

2. Materials and methods

2.1. Materials used

Rice husk was obtained from a local rice mill in the Lahore area, Pakistan. Chitosan with 92% of deacetylation degree in flake form (0.1–6 mm) was purchased from Sigma Aldrich, Pakistan and used without further purification. The chemicals used in this study, such as, nitric acid, hydrochloric acid, sodium hydroxide; all of analytical grades (98–99%) etc. were supplied from Merck. Distilled water was used for preparation of all solutions. Commercial Reactive Orange 113 (RO113) and Everzol Black Gr (EBG) were provided by Pakistan Council of Scientific and Industrial research (PCSIR) Laboratories. The chemical structures of the two dyes are given in Fig. 1.

2.2. Preparation of ZnO-coated chitosan carbonized rice husk (ZnO-CCRH) adsorbent

The rice husk was prepared following the method of Tao et. al. [29] with some minor modifications. According to the procedure, the rice husk was initially washed with distilled water and then dried for 5 h at 100°C in a hot air oven. The dried rice husk was subsequently ground and then sieved to a particle size of 0.175–0.250 mm (60–85 mesh) [30]. The rice husk was then immersed in concentrated nitric acid (1:1 by weight) and shaken in a water bath for 1.5 h at 70°C in order to reduce the silica content [31]. Acidified rice husk was kept overnight and then placed in a muffle furnace for 4 h at 600°C. The resulting carbonized rice husk (CRH) was cooled in a desiccator until further use.

ZnO-coated chitosan was prepared by dissolving 2 g of chitosan in 50 ml of 0.2M $ZnSO_4$ solution at room temperature followed by shaking on an orbital shaker for 2 h. 2 g of carbonized rice husk (CRH) was added to the ZnO-coated chitosan gel and placed on a rotary shaker for 3 h at 200 rpm. 10 ml 0.5 M NaOH solution was added to the ZnO-coated chitosan carbonized rice husk gel and left to react for 12 h. The resulting ZnO-chitosan-carbonized rice

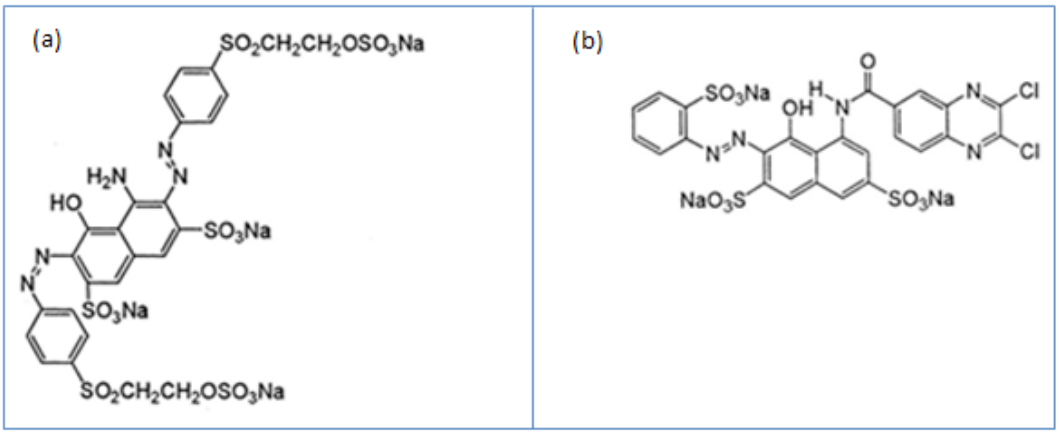

Fig. 1. Chemical Structures of dyes. a) Everzol black (reactive black 5), b) Reactive orange 113.

husk (ZnO-CCRH) composite was then rinsed with distilled water to remove excess NaOH and added to 35 ml cross linking agent i.e. 7.5% glutaraldehyde dissolved in ethanol and left to react overnight. The ZnO-CCRH adsorbent was then washed with distilled water and dried for 3 h at 100°C.

2.3. Characterization of the ZnO-CCRH adsorbent

The specific surface area of the ZnO-CCRH was estimated by sodium hydroxide titration using the method of Sears [32], yielding a value of 1.88 m^2/g. The Point of Zero Charge (PZC) of the ZnO-CCRH adsorbent was further determined by mass titration [33], yielding a pH value at the PZC of 7.15.

The presence of different functional groups and covalent bonds in the ZnO-CCRH adsorbent were analyzed using Fourier Transform Infrared spectroscopy (FTIR) while crystallinity and morphology of the adsorbent were analyzed using powder X-ray diffraction (XRD) and scanning electron microscopy (SEM), respectively.

2.4. Experimental set-up

Batch adsorption experiments were conducted in triplicate to evaluate adsorption properties of the ZnO-CCRH adsorbent with respect to sorption of Reactive orange 113 (RO113) and Everzol Black Gr(EBG). Batch adsorption experiments were conducted by adding a selected amount of adsorbent into 50 ml of stock solution containing a known concentration of dye. The solution was then adjusted to pH = 7 using either 1M HCl or NaOH. Samples were then shaken on an orbital shaker at 100 rpm for a predetermined amount of time. Samples were subsequently filtered through Whattman ash less filter paper and final dye concentrations were measured via absorbance readings at characteristic wavelengths (449 nm for RO 113, 585 nm for EBG) on a Shimadzu spectrophotometer.

2.5. Optimization of parameters

Optimization of different parameters like adsorbent dose, agitation speed, agitation time, initial concentration, pH and temperature were carried out on batch scale.

2.5.1. Effect of temperature

Temperature effects were investigated by varying the process temperature from 20°C to 80°C in 20°C increments. Additional experiments were also carried out at room temperature *i.e* 25°C. Dye solution of 20 ppm of neutral pH along with 0.075 adsorbent dose at the selected temperatures were agitated for 30 min at 100 rpm speed. After a specific time interval samples were filtered and analyzed for remaining dye concentration. The temperature was controlled using a digital water bath shaker (Nickle-Electro Lt, model: NEF-28D series).

2.5.2. Effect of adsorbent dose

In order to estimate the adsorption (decolorization) capacity of the adsorbent,different amounts of adsorbent (0.01, 0.025, 0.075, 0.10 and 0.125 g) were added to the batch adsorption experiments for both dyes. While varying adsorbent dose all other condition remained unchanged. After 30 min shaking time solutions of both dyes were filtered and analyzed for residual dye concentration.

2.5.3. Effect of shaking speed

Shaking speed has an impact on diffusion of solute contained in aqueous solution as well as development of the outer boundary layer at the adsorbent surface. Therefore, batch sorption experiments were carried out at different shaking speeds to evaluate its impacts on dye removal efficiency. Shaking speed was varied between 50 and 300 rpm in 50 rpm increments, using an orbital shaker (Stuart, model: SSL1). Experiments were carried out for each shaking speed using a 20 ppm dye solution (for both dyes) of neutral pH added with 0.075 g adsorbent dose at 25°C temperature and agitated for 30 min. After a pre-selected time interval samples were filtered and analyzed for remaining dye concentration.

2.5.4. Effect of contact time

Effect of contact time on dye removal efficiency was investigated by carrying out batch sorption experiments

with contact times of 30, 60, 90, 120, 150, 180 and 210 min for both model dyes. Experiments were carried out using a 20 ppm dye solution of neutral pH with 0.075 g adsorbent dose added. Experiments were further conducted at room temperature at a shaking speed of 100 rpm. After completion of every experiment, flask contents were removed, filtered and analyzed for remaining dye concentration.

2.5.5. Effect of pH

Effects of solution pH on dye removal efficiency was investigated using dye solutions having pH of 3, 5 7, 9 and 11. Solution pH was adjusted using either 0.1 M HCl or NaOH. A pH meter (Elico model: LI 617) was used to check the pH of the reactor solutions. During the experiments all other parameters remained unchanged. After 30 min contact time, flask contents were filtered and analyzed by spectrophotometer.

2.5.6. Effect of dye concentration

Impact of initial dye concentration on dye removal efficiency was investigated using initial dye solution concentrations of 5, 10, 15, 20, 25 and 30 ppm. All other parameters remained unchanged during the experiments. After a pre-selected time interval, flask contents were removed, filtered and analyzed on a spectrophotometer for final dye concentration determination.

2.6. Analysis

After a pre-selected agitation time, flask contents were removed and filtered through Whattman ash less filter paper. Final concentrations of Reactive Orange 113 and Everzol Black Gr were determined by measuring the absorbance at 449 nm and 585 nm, respectively, using a Spectrophotometer (Analytikjena Specord 200).

2.7. Calculations

Data acquired from the batch sorption experiments were subsequently used to determine the final dye concentrations, adsorbent adsorption capacity and adsorption isotherm characteristics, as well as kinetic and thermodynamic parameters. The relative removal dye removal was calculated as [34].

$$\%\ \text{Decolorization} = (\text{Initial absorbance} - \text{Final absorbance})/\text{Initial absorbance} * 100\% \quad (1)$$

A mass balance was used to determine the adsorption capacity of the adsorbent as [35].

$$Q = [(C_0 - C_e)/m]\, V \quad (2)$$

where Q = the amount of dye adsorbed per unit weight of adsorbent (mg/g); C_0 = Initial concentration of adsorbent solution (mg/l); C_e = Final concentration of adsorbent solution (mg/l); m = Adsorbent dosage (g); V = Volume of adsorbent solution (l).

3. Theory

3.1. Adsorption isotherms

The adsorption isotherm is significant for the explanation of how the adsorbent will interact with the adsorbate and give an idea of adsorption capacity. In this regard, the three most important isotherms: Langmuir, Freundlich and Tempkin were applied to the batch adsorption data to produce detailed information about the adsorption mechanisms for the dye adsorption process.

3.2. Langmuir isotherm

The Langmuir isotherm model is representative of mono layer sorption occurring on an energetically uniform surface on which the adsorbed molecules are not inter active. Accordingly, equilibrium is attained once the mono layer is completely saturated. The linear form of the Langmuir equation is represented as follows:

$$C_e/q_e = 1/q_m b + C_e/q_m \quad (3)$$

where q_m = Maximum capacity of adsorbent to form a complete mono layer on the surface (mg/g); C_e = Adsorbent concentration in the solution at equilibrium; q_e = Adsorbent concentration on the adsorbent at equilibrium; b = Langmuir constant related to the heat of adsorption (l/mg)

Plotting C_e/q_e vs. C_e, should yield a straight line with slope $1/q_m$ and intercept $1/q_m$ b, from which q_m and b can be determined.

The essential characteristics of the Langmuir isotherm can be expressed by a dimensionless constant called an equilibrium parameter, R_L:

$$R_L = 1/(1+ K_L C_i) \quad (4)$$

where C_i is the initial sorbate concentration and K_L is the so-called Langmuir constant that is related to the energy of adsorption [36]. Based on the value of R_L, the adsorption process can be characterized as favorable ($1 > R_L > 0$), unfavorable ($R_L > 1$) or irreversible ($R_L < 0$). A value of $R_L = 1$ indicate linear sorption. Values of fitted Langmuir sorption isotherm parameters [Eq. (3)] for adsorption of EBG and RO113 dyes on ZnO coated chitosan carbonize rice husk are given in Table 2.

3.3. Freundlich isotherm

This isotherm is an empirical equation employed to describe a heterogeneous sorption system and is expressed by the following linearized equation

$$\log q_e = \log K_f + 1/\mathrm{n} \log C_e \quad (5)$$

where K_f = Freundlich Constant (mg/g); n = Adsorption intensity measure of adsorbent molecules

A plot of log q_e vs. log C_e will yield a straight line with a slope of $1/n$ and intercept equal to $\log (K_f)$. Values of fitted Freundlich adsorption parameters for the two dyes are given in Table 2.

3.4. Temkin isotherm

Unlike the Langmuir and Freundlich isotherms, the Temkin isotherm takes into account the interactions between adsorbents and sorbates and is based on the assumption that the free energy of sorption is a function of the surface coverage. The isotherm is given as follows:

$$q_e = B_T \ln (A_T C_e) \quad (6a)$$

$$B_T = RT/b_T \quad (6b)$$

where A_T = Equilibrium binding constant corresponding to the maximum binding energy; b_T = Temkin isotherm constant; B_T = Constant related to the heat of adsorption (J/mol); T = Temperature (K); R = Ideal gas constant (8.315 J mol^{-1} K^{-1}).

4. Kinetic modeling

From kinetic analysis, it is possible to establish the adsorbent uptake rates, which in turn determines the required residence time for completion of the adsorption reaction. In this study, the pseudo-first-order, pseudo-second-order kinetic models were considered.

One of the most commonly used pseudo-first-order models also known as the Lagergren model is generally expressed as

$$\ln(q_e - q_t) = \ln q_e - K_1 t \quad (7)$$

where q_t = Mass of adsorbent adsorbed at time t (mg/g); K_l = First-order reaction rate equilibrium constant (min^{-1}).

The pseudo-second-order equation based on adsorption equilibrium capacity assumes that the rate of occupation of adsorption sites is proportional to the square of the number of unoccupied sites and may be expressed in the form

$$t/q_t = 1/K_2 q_e^2 + t/q_e \quad (8)$$

where K_2 = Second-order reaction rate equilibrium constant.

A plot of t/q_t against t should yield a linear relationship if the second-order kinetic model is applicable. Fig. 4 shows fitted kinetic models [Eqs. (7) and (8)] to the experimental data while fitted model parameters are listed in Table 4.

4.1. Thermodynamic parameters

Effect of temperature on the adsorption process can be characterized via the thermodynamic properties of the reaction. Effect of temperature on adsorption of EBG and RO 113 onto ZnO coated chitosan carbonize rice husk was thermodynamically studied and results shown in Fig. 5. Thermodynamic parameters were calculated by applying the van't Hoff equation:

$$\ln K = \Delta H^\circ/RT + \Delta S^\circ/R \quad (9)$$

where K = thermodynamic equilibrium constant.

The relationship between free energy change at standard state, (ΔG°), enthalpy change (ΔH°) and entropy change (ΔS°) for the adsorption process is expressed as

$$\Delta G^\circ = \Delta S^\circ - \Delta H^\circ \quad (10)$$

5. Results & discussion

5.1. Adsorbent structural characteristics

5.1.1. FTIR

FTIR spectra of the fresh and spent ZnO-CCRH adsorbent (after the adsorption of either EBG or RO113) are shown in Fig. 2. The changes in absorption frequencies are given in Table 1. It is seen ZnO-CCRH exhibit absorption peaks in the wave number regions 3000–3600 cm^{-1} and 800–1650 cm^{-1}. The absorbance peaks at 3522.7 cm^{-1} and 3425.72 cm^{-1} represent the presence of O-H bonds, which may be related to carboxylic or alcoholic groups. The weak and sharp absorbance peaks at 3378.24 cm^{-1}, 3330.94 cm^{-1} and 3257.61 cm^{-1} may indicate the presence of N-H groups (most probable secondary amines) associated with carbonyl, carboxylic, or ketone groups. The peaks at 3123.57 cm^{-1} and 3052.47 cm^{-1} represent = C-H , while the peaks at 1627.74 cm^{-1}, 1384.92 cm^{-1}, 1099-36 and 786.86 cm^{-1} indicate C=C, -C-H, C-O and =C-H groups respectively. After adsorption of EBG, the spectrum of ZnO-CCRH-EBG shows that the absorbance of the O-H and N-H groups have shifted to slightly higher wave numbers (3522.7 to 3551.76 cm^{-1}, 3460.56 to 3475.40 cm^{-1}, 3330.94 to 3368.31 cm^{-1} and 3257.61 to 3300.13 cm^{-1}). Two prominent absorbance peaks at 3123.57 cm^{-1} and 3052.47 cm^{-1} corresponding to =C-H stretch bonds have disappeared. New absorption peaks have appeared at 3690.31 cm^{-1}, 3590.02 cm^{-1} and 2365.71 cm^{-1} corresponding to different types of O-H bonds. These results provide strong evidence that adsorption is taking place, and that chemical changes in both sorbent and sorbate are taking place. Similar changes were also observed during adsorption of RO113. Absorption peaks for

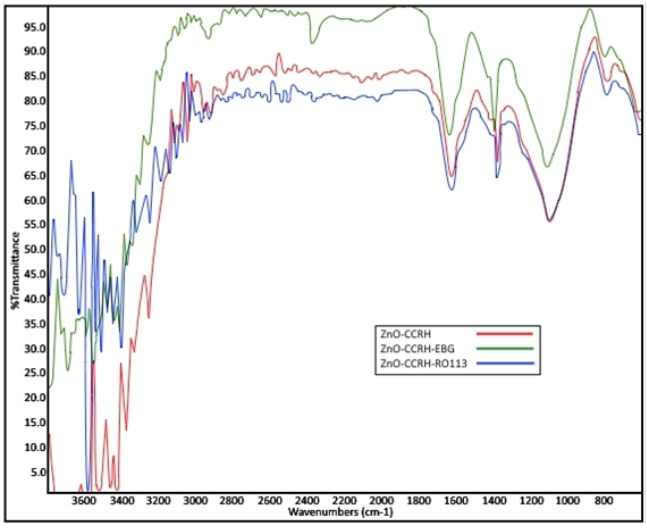

Fig. 2. FTIR spectra of ZnO-CCRH adsorbent and spent adsorbent (ZnO-CCRH-EBG, ZnO-CCRH-RO113).

Table 1
FTIR Characteristic absorption of various functional groups

Functional groups	ZnO-CCRH	ZnO-CCRH (EBG)	ZnO-CCRH (RO113)
O-H (Stretch, H-Bonded)	3522.7 cm^{-1}	3551.76 cm^{-1}	3511.32 cm^{-1}
	3460.56 cm^{-1}	3475.40 cm^{-1}	3479.08
	3425.72 cm^{-1}	Vanished	3446.39 cm^{-1}
	–	–	3518.79 cm^{-1}
	–	–	3198.88 cm^{-1}
O-H (Stretch, Free)		3690.31 cm^{-1}	–
		3590.02 cm^{-1}	–
	–	–	3710.36 cm^{-1}
	–	–	3632.52 cm^{-1}
O-H (Acid)		2365.71 cm^{-1}	–
N-H Stretch	3378.24 cm^{-1}	Vanished	3407.69 cm^{-1}
	3330.94 cm^{-1}	3368.31 cm^{-1}	–
	3257.61 cm^{-1}	3300.13 cm^{-1}	–
=C-H Stretch	3123.57 cm^{-1}	–	3110.89 cm^{-1}
	3052.47 cm^{-1}	–	3041.55 cm^{-1}
C=C, -C-H, C-O	750–1650 cm^{-1}		

O-H and N-H groups have shifted to higher wave numbers (3460.56 to 3479.08 cm^{-1}, 3425.72 to 3446.39 cm^{-1} and 3378.24 to 3407.69 cm^{-1}) or lower wave numbers (3522.7 to 3511.32 cm^{-1} and 3123.57 to 3110.89 cm^{-1}). Absorbance peaks for the =C-H and C-H groups have also shifted to higher wave numbers (3052.47 to 3041.55 cm^{-1}, 2955.23 to 2975-79 cm^{-1} and 2928.64 to 2934.05 cm^{-1}) while several new O-H group peaks have appeared (represented by absorption peaks at 3710.36 cm^{-1}, 3632.52 cm^{-1}, 3518.79 cm^{-1} and 3198.88 cm^{-1}).

The absorbance at 3518.79 cm^{-1} is very strong indicating strong adsorption effect of the adsorbent. In all three spectra in Fig. 2, the absorbance for the C=C, -C-H, C-O and =C-H groups in the wave number range of 750–1650 cm^{-1} remain unaltered indicating that these groups are unimportant for the sorption process. The changes in absorbance of spent compared to fresh adsorbents occurred at higher wave numbers (2800–3650 cm^{-1}) indicating that N-H and O-H groups are responsible for adsorption of the dyes Absorbance for ZnO-CCRH-EBG was somewhat weaker than for ZnO-CCRH-RO113 indicating that the mechanisms for removal as expected are different.

5.1.2. XRD

X-ray diffractograms for both fresh and spent ZnO-CCRH are shown in Fig. 3. None of the three diffractograms showed any larger distinct peaks indicating that the materials are generally amorphous in nature, and hence have strong adsorptive behavior. A smaller but relatively sharp peak appears at 35.79 on 2T heta scale representing the presence of Zn corresponding to the ZnO in the material. The magnitude of this peak for spent Zn-CCRH adsorbent is some what lower as compared to fresh adsorbent, indicating that Zn is active in the adsorption process. Also, some minor peaks appear at 26.65, 54.86 and 59.23 on 2 Theta scale representing the presence of silica likely associated with impurities in the rice husk. The adsorbent and spent adsorbent may possess nanomaterial characteristics because the nano related materials can cause peak broadening in diffractograms. The nanoparticle nature of the adsorbents is also supported by the SEM images (Fig. 4).

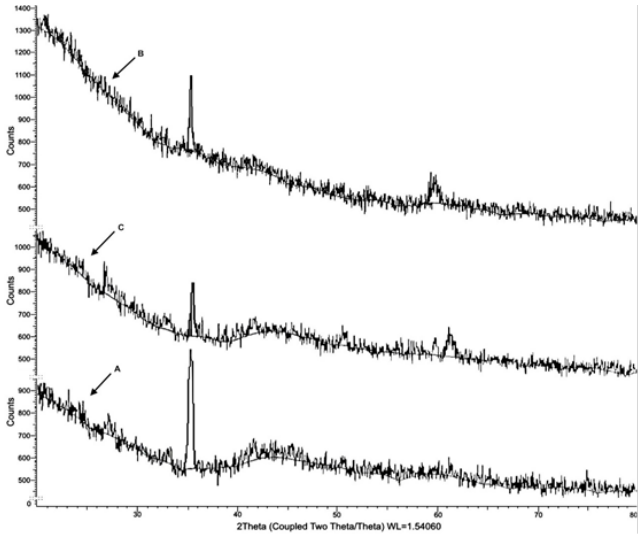

Fig. 3. (a) Diffractogram of adsorbent ZnO-CCRH with reference Pattern (b) Diffractogram of ZnO-CCRH loaded with RO113 dye (c) Diffractogram of ZnO-CCRH loaded with EBG dye.

5.1.3. SEM

SEM images of ZnO-CCRH showing surface morphology at 65, 14,000 and 30,000 times magnification. Surface texture at 65× magnification (Fig. 4a) reveals that adsorbent material particles are of irregular shape with rough surfaces and edges. At 14000 × magnification (Fig. 4b), it is seen that the material consists of thin particles ZnO-CCRH (wafers), approximately hexagonal in shape, immersed in somewhat porous and fluffy material which may be the biopolymer network of carbonized rice husk. At 30000× magnification, the particles exhibit specific geometry and loading of Zn into the insoluble biopolymer. The fluffy material of the CCRH is porous due to cross linkage of fibers, which enhances the adsorption characteristics of ZnO-CCRH. SEM images also reveal that the composite may be amorphous in nature rather than crystalline. This observation is further supported by X-ray diffraction spectrography [37].

5.2. Adsorbent efficiency characteristics

5.2.1. Langmuir isotherm behavior

For both dyes correlation coefficients (r^2) are close to 1 (0.979 for EBG and 0.998 for RO113) indicating very good fits. Table 2 also shows that the maximum adsorption capacity q_m for RO113 (=18.184 mg/g) is higher than for EBG (=13.446 mg/g). A possible explanation is that EBG is a larger molecule (mol. wt. 992 g/mol) compared to RO113 (mol. wt. 550 g/mol) and therefore may require more surface area for adsorption. In com-

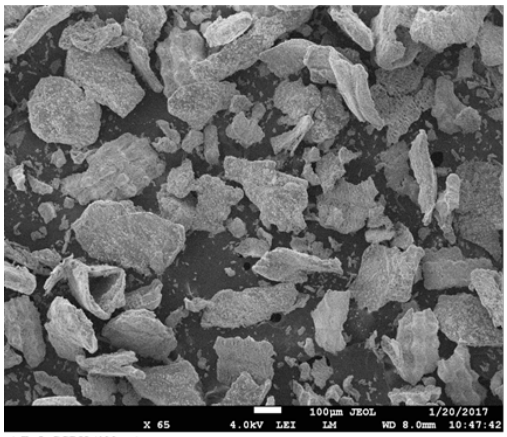

a) ZnO-CCRH (100µm)

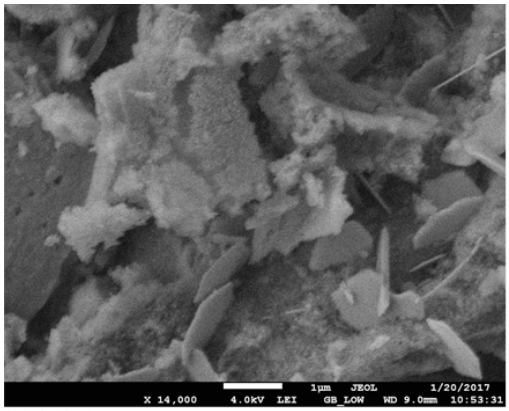

b) ZnO-CCRH (1µm)

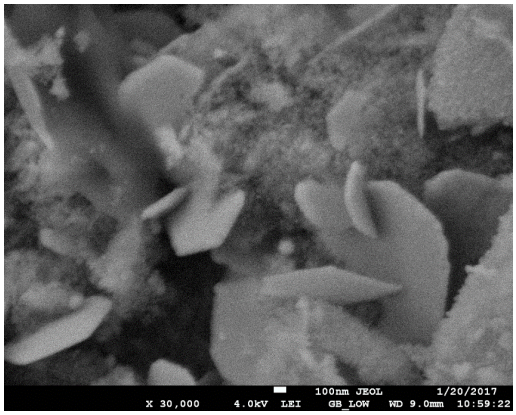

Fig. 4. SEM images of ZnO-CCRH a) 100 µm, b) 1 µm, c) 100 nm.

parison, Sugashini et al. [24] observed q_m values ranging from 4.6 to 24.5 mg/g for adsorption of Cr (VI) ions onto differently treated carbonized rice husk-based sorbents, with Fe-loaded chitosan carbonized rice husk yielding q_m = 24.5 mg/g in 25 ml 100 ppm Cr (VI) solution with 0.1 g Fe-CCRH at pH = 2.

The energy of adsorption as quantified by the factor b in Eq. (3) is higher for RO113 dye. Values of R_L for sorption of the two dyes onto ZnO coated chitosan carbonized rice husk listed in Table 3 are all very close to one ($R_L \approx 1$), indicating linear sorption of EBG and RO113.

Table 2
Langmuir, Freundlich and Temkin adsorption isotherm model parameters for of adsorption of EBG and RO113 onto ZnO coated chitosan carbonize rice husk

Model	Dye	Constants		R^2
Langmuir		q_m (mg/g)	b (L/mg)	
	Everzol Black Gr	13.446	96.994	0.979
	Reactive Orange 113	18.184	116.38	0.998
Freundlich		N	K_F (mg/g)	
	Everzol Black Gr	1.867	4.411	0.957
	Reactive Orange 113	1.859	4.714	0.967
Temkin		B_T (kJ/mol)	K_T (mg/g)	
	Everzol Black Gr	0.750	4.249	0.964
	Reactive Orange 113	0.671	4.006	0.992

Table 3
Values of the Langmuir equilibrium factor (R_L) at different initial concentrations (C_i) for the adsorption of EBG and RO113 on onto ZnO coated chitosan carbonize rice husk at different initial concentrations

C_i (mg/l)	R_L (EBG)	R_L (RO113)
5	1.01	1.01
10	1.02	1.02
15	1.03	1.03
20	1.05	1.04
25	1.06	1.05

5.2.2. Freundlich isotherm behavior

Again, very good fits (r^2 = 0.957 for EBG and 0.967 for RO 113) were obtained (Table 2). The adsorption behavior for this isotherm model can be characterized by the value of n. If $n > 1$ adsorption is a physical process (physiosorption) and favorable [38]. As shown in Table 2, values of n for the two dyes are larger than 1, indicating a favorable adsorption process. The ultimate adsorption capacity 'K_F' of EBG and RO 113 as calculated from the Freundlich isotherm is 4.411 mg/g and 1.859 mg/g respectively. The high K_F values for both EBG and RO113 indicate that these dyes effectively bonded with the adsorbent surface and that sorption occurred in more than one layer of adsorbate on the adsorbents.

5.2.3. Temkin isotherm behavior

Fitted Temkin model parameters are given in Table 2. Values of B_T that is related to the energy of adsorption are 0.750 kJ/mol and 0.671 kJ/mol for EBG and RO113 respectively. The relatively low values of B_T (<8), indicate that the interactions between the dyes and ZnO coated chitosan carbonize rice husk were relatively weak and that the adsorption of the dyes onto the ZnO coated chitosan carbonize rice husk can be expressed mainly as physiosorption [34,39] as was also indicated above by the Freundlich isotherm data.

This means that sorption occurs primarily due to van Der Waals forces and that the sorption process is reversible. This is further in agreement with the findings from the Langmuir isotherm analyses where the observed values of R_L (≈ 1) were well within the region associated with reversible adsorption.

5.3. Effect of process conditions on adsorption efficiency

5.3.1. Adsorbent dose

Effect of adsorbent dose on removal (adsorption) of the two dyes during batch equilibrium conditions is illustrated in Fig. 5a. Over the range of adsorbent doses (0.01–0.15 g adsorbent/50 ml solution) the removal efficiency increased from 10% to 92% for EBG and 5% to 88% for RO113. Although removal efficiency was slightly lower for RO113, differences between the two dyes were not significant at the 95% confidence level. It is evident that by increasing adsorbent concentration it is possible to achieve relatively high removal efficiencies. In comparison, Abd El Maksod et al. [40] found that for sorption of the dye Remazol Reactive Red 198 onto eggshells, an increase in sorbent dose from 5 to 20 g/ L increased dye removal from 38 to 65%. Fig. 4a also indicate that the maximum increase in dye removal efficiency per amount of additional adsorbent added, occur at adsorbent concentrations of 0.04 g/50 ml for EBG and 0.06 g/50 ml for RO113. From an economical point of view, these are the points where it is most cost-effective to use additional sorbent to increase removal efficiency.

5.3.2. Initial dye concentration

The effect of initial concentration of Everzol Black Gr and Reactive Orange 113 dyes on removal efficiency is shown in Fig. 5b. It is evident from the results that the removal efficiency of dyes decreases with an increase in the initial concentration of the dyes. This is to be expected due to increased competition for the available adsorption sites. Commonly, for a given dose of adsorbent the total number of accessible adsorption sites is static, thus, the maximum quantity of dye (adsorbate) that can be adsorbed remains the same. The data, however, also shows that removal efficiency does not decrease in proportion to the increase in initial dye concentration. This indicates that although increasing initial dye concentration causes increasing sorption, maxi-

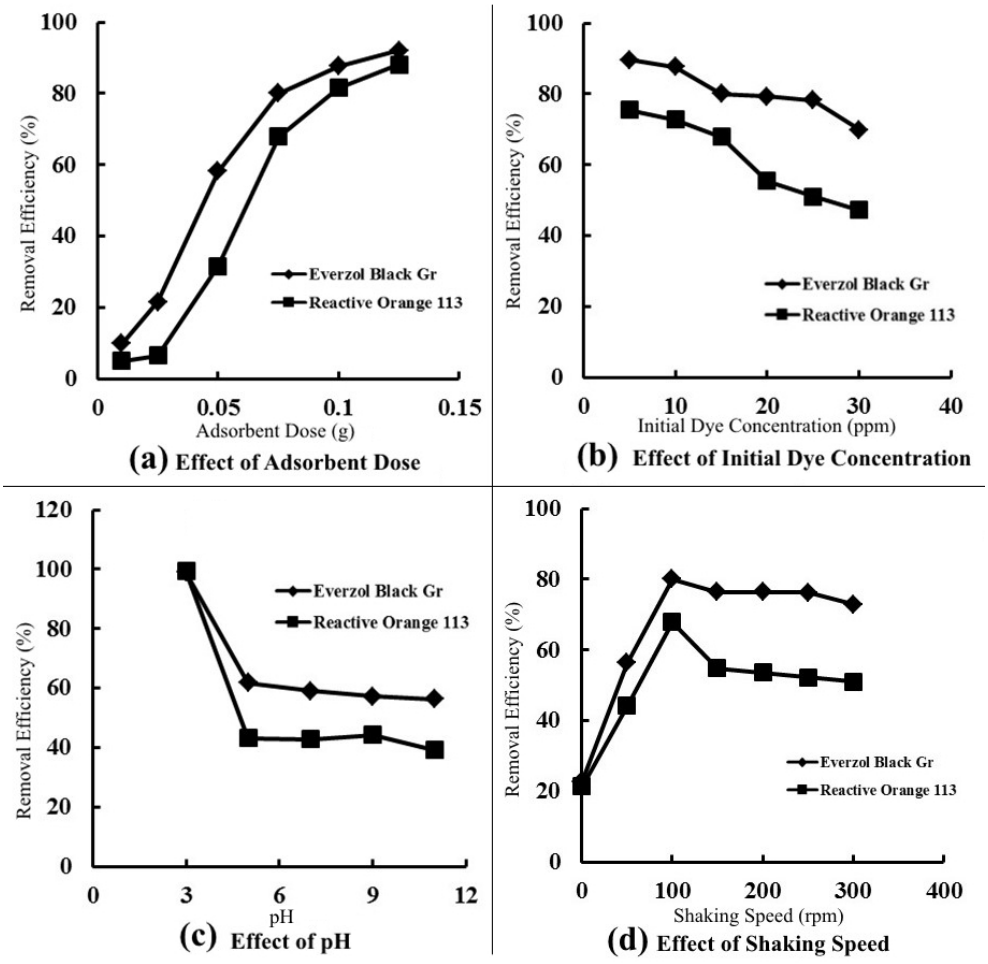

Fig. 5. Effect of Adsorbent dose, Initial Dye concentration, pH and shaking speed on removal efficiency of Reactive Orange 113 and Everzol Black Gr dyes.

mum sorption capacity is far from being reached in any of the experiments shown in Fig 4b. For the maximum initial concentration (30 mg/l) adsorbate, final adsorbed concentrations are 70% and 47% for EBG and RO113, respectively which are both well below the maximum adsorption capacity as estimated by the adsorption analyses.

5.3.3. Reaction pH

In case of physiosorption, pH is considered the most important parameter controlling the process of adsorption as it controls surface charges of both adsorbent and adsorbate, the level of ionization in the solution and the division of functional groups on the active sites of the adsorbent [18]. The effect of pH on removal efficiency of Everzol Black Gr and Reactive Orange 113 dyes is shown in Fig. 5c. The data in Fig. 4c indicate that the maximum removal efficiency for both dyes occur at relatively low pH. At pH = 3, removal efficiency of both dyes was 99%.As both dyes are basic in nature (negative surface charge), adsorption is more efficient when adsorbent surface charge is positive (i.e., at pH < PZC). The above observation is thus, consistent with the observed PZC at pH = 7.15. At pH ≥ PZC, observed dye removal efficiency is independent of pH as might be expected. [35] conducted a study on the removal of reactive dye Reactive Red 222 (RR 222) by using Epichlorohydrin cross linked chitosan (ECH) in acidic and basic pH range and also observed optimal removal efficiency at pH = 3.

5.3.4. Shaking speed

The shaking speed used during the adsorption reaction is another important parameter. Agitation affects the formation and properties (thickness and charge) of exterior boundary films on both adsorbent and adsorbate in the solution/suspension [41]. The effect of agitation level (shaking speed) on removal efficiency of dyes is shown in Fig 5d. The data in Fig. 4d show that maximum removal efficiency (80% for EBG and 68% for RO113). At shaking speeds below 100 rpm, removal efficiency increases almost linearly with increasing shaking speed. This is likely caused by reduced thickness of the boundary layers caused by increased shear forces in the liquid phase. This allows for better contact between adsorbent and adsorbate, resulting in less sorption resistance, thereby increasing removal efficiency. At shaking speeds above 100 rpm, removal efficiency decreases with increasing shaking speed at a relatively moderate rate. This behavior may be explained by increased shear forces related to turbulence and energy dissipation that disrupts the relatively weak bonds between adsorbent and adsorbate in this region, causing increased sorption resistance [42].

5.4. Kinetic modeling

The effect of contact time on EBG and RO 113 dye removal efficiency at an initial adsorbent concentration of 20 ppm is shown in Fig. 6. The results in Fig. 6 show that ZnO coated chitosan carbonized rice husk exhibits faster adsorption of EBG compared to RO113. At 120 min contact time removal efficiency was 94% for EBG and 89% for

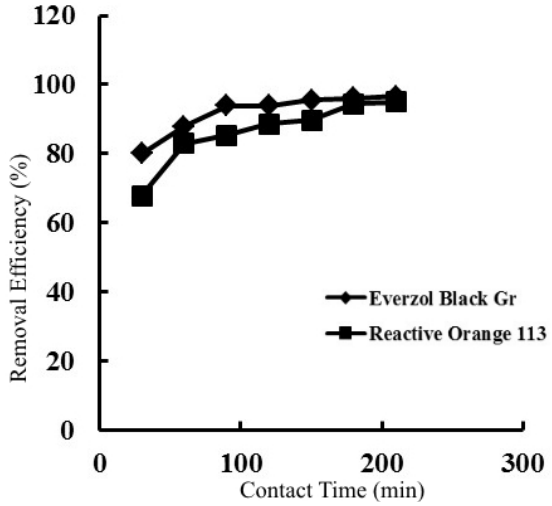

Fig. 6. Effect of contact time on removal efficiency of Everzol Black Gr and Reactive Orange 113 dyes.

Table 4
Fitted kinetic model parameters for the pseudo first-order model (Eq. (7)) and the pseudo second order model (Eq. (8)) for adsorption of EBG and RO113 onto ZnO coated chitosan carbonize rice husk

Adsorbent	Pseudo first order			Pseudo second order		
	q_e (mg/g)	K_1 (min^{-1})	r^2	q_e (mg/g)	K_2 (g mg^1 min^1)	r^2
EBG	4.5	0.023	0.97	14.3	0.0090	0.99
RO113	4.7	0.012	0.93	14.4	0.0040	0.99

RO113, while both dyes showed similar removal efficiencies at contact times above 150 min. Thus, for both dyes adsorption is not instantaneous but requires a certain contact time for effective removal to take place.

Best fit pseudo first order (Eq. (7)) and pseudo second order (Eq. (8)) model parameters to the experimental data in Fig. 6, are shown in Table 4.

Although both kinetic models fit the experimental data relatively well as indicated by the high regression r^2 values, the data indicate that the pseudo second order model [Eq. (8)] yields the best fit, indicating that the pseudo-second-order kinetic model may be used to describe the adsorption of EBG and RO113 onto ZnO coated chitosan carbonized rice husk.

5.5. Thermodynamic properties

Again, removal efficiency is higher for Everzol Black Gr compared to Reactive Orange 113 at all temperatures considered in agreement with the previous findings. For RO113, removal efficiency increases almost linearly with temperature below about 60°C while it becomes almost constant at temperatures above 60°C For EBG the same behavior is observed although removal efficiency becomes constant already at temperatures above 40°C. Part of the reason why removal efficiency increases with temperature is likely the

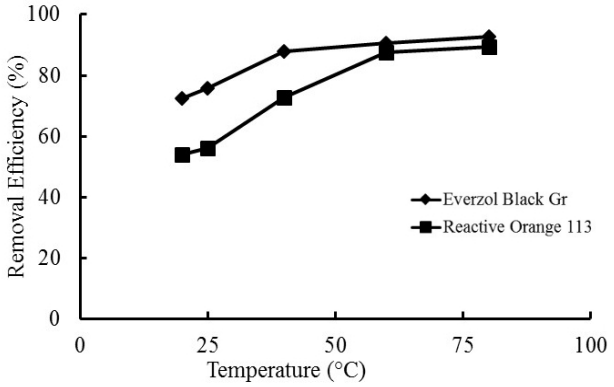

Fig. 7. Effect of temperature on removal efficiency of Everzol Black Gr (EBG) and Reactive Orange 113 (RO 113) dyes.

Table 5
Thermodynamically parameters of adsorption of EBG and RO113 on onto ZnO coated chitosan carbonize rice husk

Adsorbent	Thermodynamic parameters			
	ΔG° (kJ mol^{-1})	ΔS° (kJ mol^{-1}K^{-1})	ΔH° (kJ mol^{-1})	r^2
EBG	–0.796–(–0.22)	0.0086	–0.85	0.70
RO113	–1.5–(–0.33)	0.021	–1.85	0.90

increased mobility of the dye molecules in the liquid phase due to increased diffusion coefficients. Increasing temperature also causes swelling of the internal structure of the chitosan, thereby exposing additional sorption sites, which in turn facilitates faster removal from the liquid phase.

Fitted values of the thermo dynamic parameters, i.e., ΔG°, ΔS° ΔH° for the two sorption processes are listed in Table 5.

The negative values of ΔG° indicated that the adsorption process was spontaneous with the highest preference of RO113 by ZnO coated chitosan carbonize rice husk at standard state. The positive values of ΔS° might show release of water molecules from hydrated shells of sorbed species that imparted randomness or uncertainty to the adsorption system. The negative values of ΔH° further indicated an exothermic adsorption process for both the dyes at standard state.

6. Conclusions

Activated carbon is the most widely used adsorbent to treat wastewater containing dyes due to its easily avail ability and extreme efficiency. However, due to the cost of regeneration or generation of activated carbon this adsorbent is now often substituted with natural, environmental friendly, low cost bio-sorbents. In this study, an alternative bio-sorbent, ZnO-coated chitosan carbonized rice husk (ZnCCRH), was evaluated with respect to its ability to remove two dyes Reactive Orange 113 (RO113) and Everzol Black, Gr (EBG) from waste water. XRD and FTIR analyses of the adsorbent material indicated that several different functional groups were active in the adsorption of the two dyes. Adsorption of both dyes was further most effective at low pH. Results further indicate that adsorption of the two dyes onto Zn CCRH is characterized by non-spontaneous, reversible physiosorption, and that multiple layers of the adsorbate is formed on the surfaces of the adsorbent. This indicates further that efficient regeneration of the sorbent is possible. Adsorption data for both dyes further indicated that sorption equilibrium could be best described by the Langmuir isotherm model (despite being multilayer sorption). Sorption kinetics for both dyes was best described by the pseudo second order model. Analyses of the thermodynamic properties of the two adsorption processes revealed that both processes were spontaneous and exothermic at standard state. In general, the results revealed that the adsorption potential of the ZnO-CCRH for RO113 and EBG dyes is very high and that removal efficiencies near 100% easily be achieved, suggesting ZnO-CCRH as a viable alternative to activated carbon when it comes to treating wastewater from the textile industry.

Acknowledgment

Authors express the sincere recognition to the staff of Center for Environmental Protection Studies (CEPS), PCSIR laboratories for their support and providing lab facilities during analyses.

References

[1] Č. Novotný, N. Dias, A. Kapanen, K. Malachová, M. Vándrovcová, M. Itävaara, N. Lima, Comparative use of bacterial, algal and protozoan tests to study toxicity of azo-and anthraquinone dyes, Chemosphere, 63 (2006) 1436–1442.
[2] Y. Wong, Y. Szeto, W. Cheung, G. McKay, Adsorption of acid dyes on chitosan—equilibrium isotherm analyses, Process Biochem., 39 (2004) 695–704.
[3] W.X. Liu, Y.P. Chao, X.Q. Yang, H.B. Bao, S.J. Qian, Biodecolorization of azo, anthraquinonic and triphenylmethane dyes by white-rot fungi and a laccase secreting engineered strain, J. Ind. Microbiol. Biotechnol., 31(3) (2004) 127–132.
[4] J. Gandhi, R. Dangi, J.C. Sharma, N. Verma, S. Bhardwaj, Photo catalytic bleaching of malachite green and brilliant green dyes using ZnS-CdS as semiconductor: A comparative study, Der Chemica Sinica., 1(3) (2010) 77–83.
[5] J. Fan, Y. Guo, J. Wang, M. Fan, Rapid decolorization of azo dye methyl orange in aqueous solution by nanoscale zerovalent iron particles, J. Hazard. Mater., 166 (2009) 904–910.
[6] A.K. Verma, R.R. Dash, P. Bhunia, A review on chemical coagulation/flocculation technologies for removal of colour from textile waste waters, J. Environ. Manage., 93 (2012) 154–168.
[7] S. Netpradit, P. Thiravetyan, S. Towprayoon, Adsorption of three azo reactive dyes by metal hydroxide sludge: effect of temperature, pH, and electrolytes, J. Colloid Interf. Sci., 270 (2004) 255–261.
[8] N. Koprivanac, A.L. Božić, S. Papić, Cleaner production processes in the synthesis of blue anthraquinone reactive dyes, Dyes Pigments., 44 (1999) 33–40.
[9] L. Monser, N. Adhoum, Modified activated carbon for the removal of copper, zinc, chromium and cyanide from wastewater, Sep. Purif. Technol., 26 (2002) 137–146.
[10] A. Demirbas, Agricultural based activated carbons for the removal of dyes from aqueous solutions: a review, J. Hazard. Mater., 167 (2009) 1–9.
[11] J.M. Dias, M.C. Alvim-Ferraz, M.F. Almeida, J. Rivera-Utrilla, M. Sánchez-Polo, Waste materials for activated carbon prepa-

ration and its use in aqueous-phase treatment: a review, J. Environ. Manage., 85 (2007) 833–846.
[12] V. Gupta, Application of low-cost adsorbents for dye removal–A review, J. Environ. Manage., 90 (2009) 2313–2342.
[13] J.-R. Jeon, E.-J. Kim, Y.-M. Kim, K. Murugesan, J.-H. Kim, Y.-S. Chang, Use of grape seed and its natural polyphenol extracts as a natural organic coagulant for removal of cationic dyes, Chemosphere, 77 (2009) 1090–1098.
[14] C.P. Sekhar, S. Kalidhasan, V. Rajesh, N. Rajesh, Bio-polymer adsorbent for the removal of malachite green from aqueous solution, Chemosphere, 77 (2009) 842–847.
[15] M.H. Entezari, Z.S. Al-Hoseini, N. Ashraf, Fast and efficient removal of Reactive Black 5 from aqueous solution by a combined method of ultrasound and sorption process, Ultrason. Sonochem., 15(4) (2008) 433–437.
[16] W.N.M. Saeed, Removal of Azo Dye Reactive Black 5 By Adsorption onto ZnO and CaO, J. Kerbala Univ., 11(4) (2013) 321–330.
[17] B.H. Hameed, A.M. Din, A.L. Ahmad, Adsorption of methylene blue onto bamboo-based activated carbon: kinetics and equilibrium studies, J. Hazard. Mater., 141(3) (2007) 819–825.
[18] G. Crini, P.-M. Badot, Application of chitosan, a natural aminopolysaccharide, for dye removal from aqueous solutions by adsorption processes using batch studies: A review of recent literature, Prog. Polym. Sci., 33 (2008) 399–447.
[19] M. Rinaudo, Chitin and chitosan: properties and applications, Prog. Polym. Sci., 31 (2006) 603–632.
[20] M.-S. Chiou, G.-S. Chuang, Competitive adsorption of dye metanil yellow and RB15 in acid solutions on chemically cross-linked chitosan beads, Chemosphere, 62 (2006) 731–740.
[21] B. Geng, Z. Jin, T. Li, X. Qi, Kinetics of hexavalent chromium removal from water by chitosan-Fe0 nanoparticles, Chemosphere, 75 (2009) 825–830.
[22] A. Shafaei, F.Z. Ashtiani, T. Kaghazchi, Equilibrium studies of the sorption of Hg (II) ions onto chitosan, Chem. Eng. J., 133 (2007) 311–316.
[23] H. Jaman, D. Chakraborty, P. Saha, A study of the thermodynamics and kinetics of copper adsorption using chemically modified rice husk, CLEAN–Soil Air Water, 37 (2009) 704–711.
[24] S. Sugashini, K.M.M.S. Begum, Adsorption and desorption studies on the performance of Fe–loaded chitosan carbonized rice husk for metal ion removal, Desal. Water. Treat., 51 (2013) 7764–7774.
[25] E.L. Foletto, D.S. Paz, A. Cancelier, G.C. Collazzo, M.A. Mazutti, S.L. Jahn, Use of rice hull as a biomass sorbent for organic pollutant removal: adsorption isotherms and thermodynamic, Latin Amer. Appl. Res., 43(1) (2013) 1–5.
[26] M. Ahmaruzzaman, V.K. Gupta, Rice husk and its ash as low-cost adsorbents in water and wastewater treatment, Ind. Eng. Chem. Res., 50(24) (2011) 13589–13613.
[27] M.A. Rahman, S.R. Amin, A.S. Alam, Removal of methylene blue from waste water using activated carbon prepared from rice husk, Dhaka Univ. J. Sci., 60 (2012) 185–189.
[28] V. Sivakumar, M. Thirumarimurugan, A. Xavier, A. Sivalingam, T. Kannadasan, Colour removal of direct red dye effluent by adsorption process using rice husk, Int. J. Biosci. Biochem. Bioinfo., 2 (2012) 377.
[29] Y. Tao, L. Ye, J. Pan, Y. Wang, B. Tang, Removal of Pb (II) from aqueous solution on chitosan/TiO_2 hybrid film, J. Hazard. Mater., 161 (2009) 718–722.
[30] V. Vadivelan, K.V. Kumar, Equilibrium, kinetics, mechanism, and process design for the sorption of methylene blue onto rice husk, J. Colloid Interface Sci., 286 (2005) 90–100.
[31] M. Sindhu, K.M. Meera, S. Begum, S. Sugashini, A comparative study of surface modification in carbonized rice husk by acid treatment, Desal. Water. Treat., 45 (2012) 170–176.
[32] G.W. Sears, Determination of specific surface area of colloidal silica by titration with sodium hydroxide, Anal. Chem., 28 (1956) 1981–1983.
[33] S. Žalac, N. Kallay, Application of mass titration to the point of zero charge determination, J. Colloid Interface Sci., 149 (1992) 233–240.
[34] M. Hossain, H.H. Ngo, W. Guo, T. Nguyen, Removal of copper from water by adsorption onto banana peel as bioadsorbent, Int. J. Geomate., 2 (2012) 227–234.
[35] M. Chiou, H. Li, Adsorption behavior of reactive dye in aqueous solution on chemical cross-linked chitosan beads, Chemosphere, 50 (2003) 1095–1105.
[36] A. Dada, A. Olalekan, A. Olatunya, O. Dada, Langmuir, Freundlich, Temkin and Dubinin–Radushkevich isotherms studies of equilibrium sorption of Zn^{2+} unto phosphoric acid modified rice husk, IOSR J. App. Chem., 3 (2012) 38–45.
[37] M. AbdElhady, Preparation and characterization of chitosan/zinc oxide nanoparticles for imparting antimicrobial and UV protection to cotton fabric, Int. J. Carbohyd. Chem., (2012) http://dx.doi.org/10.1155/2012/840591 (Article ID 840591).
[38] V. Vimonses, S. Lei, B. Jin, C.W. Chow, C. Saint, Adsorption of congo red by three Australian kaolins, Appl. Clay. Sci., 43 (2009) 465–472.
[39] J. Anwar, U. Shafique, M. Salman, A. Dar, S. Anwar, Removal of Pb(II) and Cd(II) from water by adsorption on peels of banana, Bioresour. Technol., 101 (2010) 1752–1755.
[40] I.H. Abd El Maksod, H.M. AlBishri, A.S. Al-bogami, Saudi Arabian White Silica as a Good Adsorbent for Pollutants, CLEAN–Soil, Air, Water, 42 (2014) 480–486.
[41] A. Krysztafkiewicz, S. Binkowski, T. Jesionowski, Adsorption of dyes on a silica surface, Appl. Surf. Sci., 199 (2002) 31–39.
[42] Y.-S. Ho, C.-C. Chiang, Y.-C. Hsu, Sorption kinetics for dye removal from aqueous solution using activated clay, Sep. Sci. Technol., 36 (2001) 2473–2488.